

Highly sensitive luminescence detection of photosensitized singlet oxygen within photonic crystal fibre

Gareth O.S. Williams^[a], Tijmen G. Euser^[b,c], Philip St.J. Russell^[b], Alexander J. MacRobert^{*[d]} and Anita C. Jones^{*[a]}

Abstract: Highly sensitive, quantitative detection of singlet oxygen ($^1\text{O}_2$) is required for the evaluation of newly developed photosensitizers and the elucidation of the mechanisms of many processes in which singlet oxygen is known, or believed, to be involved. The direct detection of $^1\text{O}_2$, via its intrinsic phosphorescence at 1270 nm, is challenging because of the extremely low intensity of this emission, coupled with the low quantum efficiency of currently available photodetectors at this wavelength. We introduce hollow-core photonic crystal fibre (HC-PCF) as a novel optofluidic modality for photosensitization and detection of $^1\text{O}_2$. We report the use of this approach to achieve highly sensitive detection of the luminescence decay of $^1\text{O}_2$, produced using two common photosensitizers, Rose Bengal and Hypericin, within the 60- μm diameter core of a 15-cm length of HC-PCF. We demonstrate the feasibility of directly detecting sub-picomole quantities of $^1\text{O}_2$ using this methodology, and identify some aspects of the HC-PCF technology that can be improved to yield even higher detection sensitivity.

Introduction

Singlet oxygen ($^1\text{O}_2$), the highly reactive first excited state of molecular oxygen, is important in a number of biological processes, including cell death and cell signalling, is involved in the degradation of synthetic polymers, and finds wide-ranging

applications, including cancer therapy, synthetic chemistry and waste-water treatment.^[1,2] The most common method of generation of $^1\text{O}_2$ is via photosensitization,^[3] where the triplet excited state of an optically excited sensitizer molecule undergoes electronic energy transfer to the triplet ground state of oxygen. Photosensitized production of $^1\text{O}_2$ is used to great benefit in photodynamic therapy (PDT), which harnesses the destructive power of $^1\text{O}_2$ to exert selective cytotoxic activity toward malignant cells, for the treatment of cancer.^[4-6] In addition to cancer therapy, the photodynamic effect (the damage of living tissue by the combination of a photosensitizer, light, and oxygen) is employed in the treatment of age-related macular degeneration,^[7] the sterilisation of blood components^[8] and the development of light-activated anti-microbials to combat the spread of infection by antibiotic-resistant bacteria.^[9, 10]

The wealth of applications of $^1\text{O}_2$ drives the development of new and improved photosensitizers, such as those with high two-photon absorption cross-sections to enable enhanced tissue penetration and spatial selectivity in PDT, through the use of two-photon excitation,^[11-14] or those suitable for incorporation in polymer films for anti-microbial coatings.^[9] Highly sensitive, quantitative detection of $^1\text{O}_2$ is required for the evaluation of newly developed photosensitizers and the elucidation of the mechanisms of many processes in which singlet oxygen is known, or believed, to be involved. Arguably, the most definitive test for the presence of singlet oxygen is the time-resolved measurement of its phosphorescence decay at 1270 nm. However, the extremely low intensity of this emission (quantum yield of 10^{-5} to 10^{-7} , depending on local environment), coupled with the low quantum efficiency of currently available photodetectors at this wavelength, make this a challenging and often impractical approach. The advent of sensitive NIR photomultipliers combined with photon-counting has led to an improvement over previous techniques, but the photocathode quantum efficiencies at 1270 nm are still relatively low at around 3%.^[15] Progress is being made in the development of new detector technologies, such as superconducting nanowire single-photon detectors (SNSPDs)^[16] and semiconductor-based single-photon avalanche diodes (SPADs)^[17,18], that promise substantially higher quantum efficiency, but these are still at the prototype stage. At present, the highest detection sensitivity is offered by indirect methods, using fluorescent or chemiluminescent probes, but these methods may lack selectivity if the probe responds to other reactive oxygen species, and may perturb the system as a result of the addition of an extraneous species.^[2,19-22] Typically these methods are quoted to be capable of detection of $^1\text{O}_2$ at concentrations in the nanomolar range, although a detection limit as low as 0.5 pM $^1\text{O}_2$

[a] Dr. G.O.S. Williams, Prof. A.C. Jones
EaStCHEM School of Chemistry
Joseph Black Building
The University of Edinburgh
Edinburgh, EH9 3FJ, UK.
E-mail: a.c.jones@ed.ac.uk

[b] Dr. T.G. Euser, Prof. P. St.J. Russell
Max-Planck Institute for the Science of Light
Staudtstr 2
91058 Erlangen, Germany.

[c] Dr. T.G. Euser
NanoPhotonics Centre
Cavendish Laboratory
University of Cambridge
J. J. Thomson Avenue
Cambridge CB3 0HE, UK.

[d] Prof. A.J. MacRobert
Division of Surgery & Interventional Science
University College London
Charles Bell House
London W1WJN, UK.
E-mail: a.macrobert@ucl.ac.uk

Supporting information for this article is given via a link at the end of the document.

has been estimated for a selective “trap-and-trigger” chemiluminescent probe.^[20]

We describe here a new approach to the direct, time-resolved detection of $^1\text{O}_2$ luminescence in which we exploit the unique optofluidic properties of hollow-core photonic crystal fibre (HC-PCF).^[23, 24] In HC-PCF, light is trapped in the hollow core by the surrounding 2D periodic ‘photonic crystal’ cladding, consisting of microscopic hollow capillaries running along the entire length of the glass fibre, as illustrated in Figure 1. This allows the infiltration of a sample solution (in the present case, the photosensitizer solution) into the hollow core, which is typically 10's of μm in

solution is subject to intense and homogeneous excitation along the entire length of the fibre core, resulting in efficient generation of $^1\text{O}_2$ from a sub-microlitre volume of photosensitizer; (ii) the $^1\text{O}_2$ luminescence is collected over the entire excitation path length and guided to the end of the fibre for detection. We demonstrate here the feasibility of directly detecting sub-picomole quantities of $^1\text{O}_2$, using this methodology. However, the use of HC-PCF in this application is not without its challenges and we identify some improvements that can be made to the technology to yield even higher detection sensitivity.

Results and Discussion

Figure 2 shows the phosphorescence decays of singlet oxygen produced by excitation of 0.1 μM solutions of Rose Bengal (RB) in D_2O (Figure 2(a)) and CD_3OD (Figure 2(b)), within the core of the PCF. The volume of solution contained within the 15-cm length of PCF was 0.4 μL , which equates to 40 femtomoles of the photosensitizer. As shown in Figure 2(c), addition of sodium azide (10 mM) completely quenched the observed emission, confirming that it was indeed due to singlet oxygen.^[29]

For RB in D_2O , two exponential components were required to fit the measured decays. The fitted lifetimes and fractional amplitudes are given in Table 1. The observation of two decay

Table 1. Decay times (τ) and corresponding fractional amplitudes (A_i) for the phosphorescence decay of $^1\text{O}_2$ produced by three different photosensitizer solutions in the core of the HC-PCF. The number-average lifetime, $\langle\tau\rangle$, is also given.

Sensitizer	$\tau_1 / \mu\text{s}$	$\tau_2 / \mu\text{s}$	$\tau_3 / \mu\text{s}$	A_1	A_2	A_3	$\langle\tau\rangle / \mu\text{s}$
RB in D_2O	68	5.8	-	0.17	0.83	-	16
RB in CD_3OD	200	4.2	28	0.05	0.74	0.21	19
Hyp in CD_3OD	250	5.0	34	0.05	0.74	0.21	23

components can be attributed to the production of $^1\text{O}_2$ by two distinct populations of photosensitizer, one in the bulk of the solution and one in close proximity to the silica surface surrounding the hollow core of the fibre. For the latter population, the $^1\text{O}_2$ luminescence would be efficiently quenched at the surface, giving rise to a much shorter lifetime than that of $^1\text{O}_2$ generated in bulk solution. The longer lifetime of 68 μs is in excellent agreement with numerous previous reports of values of $^1\text{O}_2$ lifetime (τ_A) of 67 or 68 μs measured in conventional cuvette-based measurements.^[27,30] The shorter lifetime of 5.8 μs is comparable in magnitude to the τ_A of 2.5 μs that was measured for $^1\text{O}_2$ adsorbed on the surface of TiO_2 in D_2O .^[31] The fractional amplitude of the short decay component indicates that a large majority, about 85%, of the $^1\text{O}_2$ is produced sufficiently close to the fibre surface to be rapidly quenched, and hence that a large fraction of photosensitizer molecules are adsorbed to the surface. This is perhaps not surprising, in view of the very large surface-area-to-volume ratio of the fibre core, $6.6 \times 10^4 \text{ m}^{-1}$. Similar behaviour has been observed previously for methylene blue in a hollow-core PCF, where 78% of the molecules in a 0.4 μM solution were found to have adsorbed on the surface; this was determined from the depletion in the optical absorbance of the

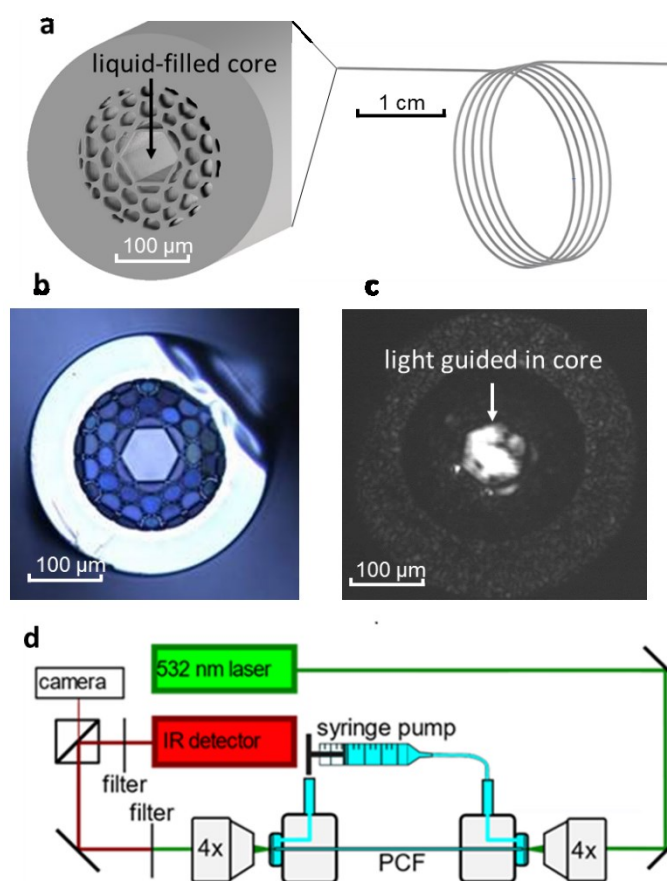


Figure 1. (a) Schematic illustration of a hollow-core photonic crystal fibre. (b) Image of the end-face of the large-core HC-PCF used in this study; this is a kagomé-type HC-PCF, named after the particular lattice arrangement in the cladding structure. (c) Image of the end face of the HC-PCF, showing confinement of the 532-nm laser beam to the core region. (d) Schematic diagram of the experimental system.

diameter, while maintaining the high optical transmission efficiency of the fibre. The confinement of both excitation light and sample solution within the core of the HC-PCF results in intense light-matter interactions over very long path-lengths ($> 10\text{cm}$), that can be exploited for chemical sensing and photochemical applications.^[23, 25, 26] As an optofluidic system for $^1\text{O}_2$ detection, HC-PCF offers two significant advantages: (i) the photosensitizer

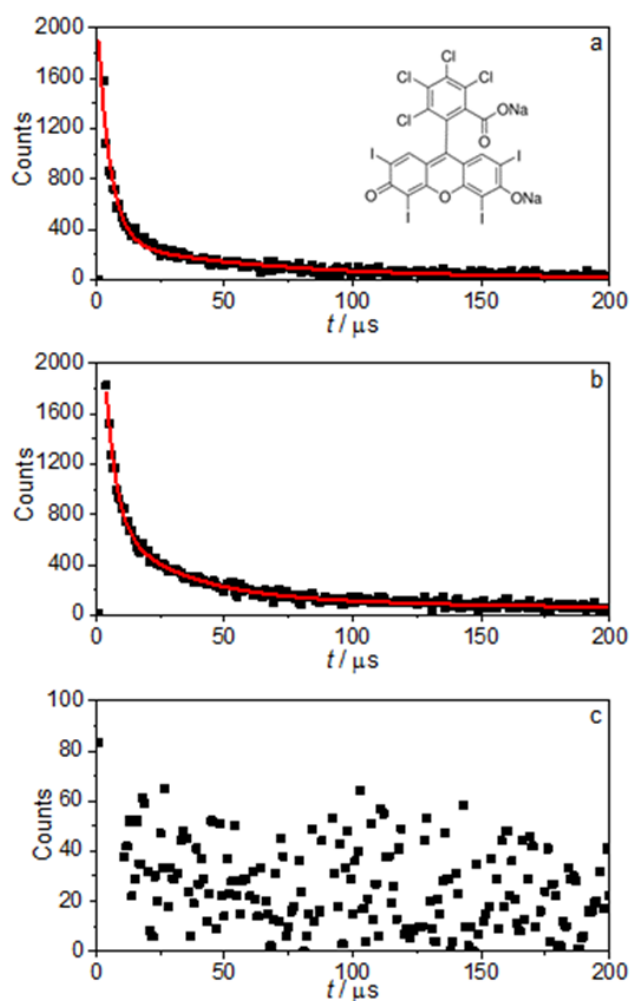


Figure 2. Phosphorescence decays of singlet oxygen produced by excitation of 0.1 μM solutions of Rose Bengal (structure shown in panel (a)) within the core of the PCF. (a) Rose Bengal in D_2O ; (b) Rose Bengal in CD_3OD ; (c) Rose Bengal CD_3OD after the addition of sodium azide at 10 mM. Experimental data are shown by black points and the fitted decay functions by red curves. The acquisition time was 1 minute.

fundamental guided mode which was confined to the solution in the body of the core.^[32] The large contribution to $^1\text{O}_2$ generation that we observe from photosensitizer on, or near, the core surface is related to the rather poor mode quality of the guided light, with the presence of higher order modes leading to relatively high excitation intensity far from the centre of the core (Figure 1(c)). (If the excitation were confined to a fundamental mode, whose intensity distribution about the centre of the core is well-approximated by the square of the zeroth-order Bessel function of the first kind with a zero value at the core boundary, we would expect to observe only photosensitization of bulk solution). The question then arises as to whether the adsorbed RB molecules are likely to be in a monomeric or aggregated state, since aggregation may affect the photosensitization efficiency. Assuming that ~85% of solute molecules are adsorbed on the

surface of the fibre core, which has an area of $2.8 \times 10^{-5} \text{ m}^2$, the average distance between adsorbed molecules will be about 35 nm. Therefore, it seems likely that the adsorbed species will be largely in monomeric form. Moreover, a previous study of the adsorption of RB on silica nanoparticles^[33] indicated that the negative charge on the silica surface in aqueous solution^[34] inhibited aggregation of the adsorbed molecules, and only the monomer was present.

The $^1\text{O}_2$ phosphorescence decay observed for RB in CD_3OD is more complex than that seen in D_2O , and requires three exponential components to give a satisfactory fit. The fitted decay parameters are shown in Table 1. This more complex decay behaviour can be rationalised in terms of an additional decay channel due to diffusion of $^1\text{O}_2$ from the body of the solution to the surface of the core. Since τ_A in CD_3OD is much longer than in D_2O , and the diffusion coefficient of O_2 is also greater, by a factor of about 2, in CD_3OD compared to D_2O ^[35] (see ESI for further details), a significant fraction of $^1\text{O}_2$ molecules produced in bulk solution can diffuse to the surface, within the excited state lifetime, and suffer quenching. In this case, the $^1\text{O}_2$ phosphorescence would be expected to show a distribution of lifetimes that reflects the spatial distribution of photosensitization within the core.

The 4.2- μs decay component (τ_2), which is very similar in lifetime and amplitude to the 5- μs component in D_2O , can be attributed to photosensitization at the surface. The similarity of the fractional amplitudes of this component in the two solvents suggests that the extent of surface adsorption is little affected by the change of solvent. The two longer decay components (τ_1 and τ_3) are presumed to approximately represent the distribution of lifetimes of $^1\text{O}_2$ produced in solution. The longest lifetime (τ_1), 200 μs , is longer than that seen in D_2O , as expected from the known solvent-dependence of τ_A ,^[27] and comparable to values of τ_A in CD_3OD that have been reported from conventional cuvette-based measurements; Bregnhøj et al. recently reported a value of 275 μs ^[27] and values reported previously include 270 μs ,^[30] 240 μs ,^[30] 288 μs and 220 μs .^[36] However, in the PCF, this unquenched component represents only about 20% of the $^1\text{O}_2$ produced in solution. The vast majority of the $^1\text{O}_2$ detected in solution is highly quenched, with an average lifetime of 28 μs , and must have been produced within diffusion distance of the core surface. The diffusion length, d_A , of $^1\text{O}_2$ can be estimated, using equation (3)^[1].

$$d_A = \sqrt{6tD} \quad (3)$$

where t is the diffusion time, which is taken to be $5\tau_A$, and D is the diffusion coefficient. For $^1\text{O}_2$ in CD_3OD , $D = 4.3 \times 10^{-9} \text{ m}^2\text{s}^{-1}$ (see ESI).

This gives a value of about 6 μm , which implies that about 36%, of the volume of photosensitizer solution would lie within diffusion distance of the core surface. This is significantly less than our estimate from the decay parameters that about 80% of the luminescence originates from $^1\text{O}_2$ molecules produced within diffusion distance of the surface. The discrepancy is likely due to the presence of higher order modes in the guided light, both the excitation light, as discussed above, and the emission. The mode properties of the guided near-infrared luminescence have not been characterised, but our results suggest that luminescence

generated near the perimeter of the core may be guided more efficiently than that produced near the centre. It may also be the case that we are underestimating the diffusion length of $^1\text{O}_2$. The phosphorescence decay of $^1\text{O}_2$ produced by excitation of 0.2 μM Hypericin (equivalent to 80 fmole in the excitation volume) in CD_3OD is shown in Figure 3. Again, a tri-exponential decay was observed, and the decay parameters (Table 1) are essentially the same as those observed for $^1\text{O}_2$ generated by excitation of RB in the same solvent. The lifetime of the longer decay component is slightly greater than was observed using RB as the photosensitizer. This can be attributed to changes in the structure of the guided excitation mode, and hence in the spatial distribution of photosensitization, between experiments. The similarity of the fractional amplitude of the 5- μs component between the two photosensitizers implies that they have similar propensity for surface adsorption.

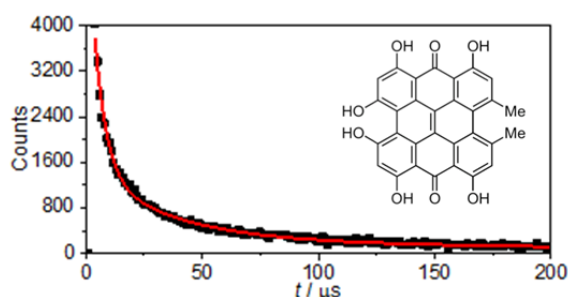


Figure 3. Phosphorescence decay of singlet oxygen produced by excitation of 0.2 μM Hypericin (structure shown) in CD_3OD , within the core of the HC-PCF. Experimental data are shown by black points and the fitted tri-exponential function by the red curve.

A potential advantage of studying photochemistry in HC-PCFs is that the precise knowledge of the excitation intensity and probed volume facilitates the measurement of absolute photochemical quantum yields, as we have shown previously.^[26] However, in the present experiments, the poor quality of the excitation mode prevented the determination of absolute quantum yields of $^1\text{O}_2$ production (Φ_A). Nevertheless, the relative values of Φ_A for the three photosensitizer systems were measured and are in good agreement with literature values,^[37] as shown in Table 2.

Table 2. The relative quantum yields for production of $^1\text{O}_2$ (Φ_A) for three different photosensitizer solutions in the core of the HC-PCF, in comparison with literature values from cuvette-based measurements. (The absolute value of Φ_A for RB in D_2O is 0.78.^[37])

Sensitizer	Φ_A relative to RB in D_2O	
	This work	Literature ^[37]
RB in D_2O	1.00	1.00
RB in CD_3OD	1.07	1.05
Hyp in CD_3OD	0.96	0.97

On the basis of the average phosphorescence lifetimes (Table 1), it is evident that the overall phosphorescence quantum yield of

$^1\text{O}_2$ in the HC-PCF is substantially lower than in bulk solution, by a factor of about four in D_2O and by an order of magnitude in CD_3OD . The surface-quenching of $^1\text{O}_2$ in the HC-PCF tends to over-ride the benefits of using deuterated solvents. The average lifetimes measured here in D_2O , 16 μs , compares with 3.5 μs in bulk H_2O ,^[27] and the average lifetime of ~ 20 μs in CD_3OD is only about twice the value of 9.5 μs in bulk CH_3OH .^[27] In spite of the undesirably efficient quenching, the detection sensitivity of $^1\text{O}_2$ luminescence within the HC-PCF remains impressively high. The 0.1 μM concentration of photosensitizer used in these measurements compares very favourably with typical concentrations of around 10 μM that are used in cuvette-based measurements of $^1\text{O}_2$ luminescence. However, a more meaningful figure-of-merit is the quantity of $^1\text{O}_2$ that can be detected. The 0.4 μL of solution contained in the fibre core amounts to 40 fmole of photosensitizer. Assuming that all of the sensitizer is excited and taking Φ_A for RB in D_2O to be 0.78, the amount of $^1\text{O}_2$ produced is 31 fmole. On the basis of the signal-to-noise ratio of the decay data (Figures 2 and 3) we estimate that a decrease in signal intensity of an order of magnitude could be accommodated, giving a limit-of-detection of 3 fmole $^1\text{O}_2$. In cuvette-based measurements, detection limits are not usually quoted in terms of amount of $^1\text{O}_2$ (or photosensitizer), presumably because of the difficulty in quantifying the detection volume. For the purpose of comparison, we will assume that a reasonable lower limit for the measurement volume is 10 μL , the volume of 1 mm x 1 mm x 10 mm microcuvette. On this basis, the detection sensitivities that are achieved typically are: ~ 100 pmole of $^1\text{O}_2$, using direct detection of $^1\text{O}_2$ luminescence; ~ 10 fmole of $^1\text{O}_2$, for more sensitive, indirect methods using fluorescent probes;^[2] and <1 fmole of $^1\text{O}_2$, for the most sensitive, indirect detection using chemiluminescent probes.^[2, 20] Thus, the sensitivity achieved by direct detection in HC-PCF is exceeded only by the most sensitive indirect methods that quantify $^1\text{O}_2$ concentration by the rate of reaction of with a chemiluminescent probe.

Conclusions

We have demonstrated that HC-PCF shows great promise as an optofluidic system for the highly sensitive quantitation of $^1\text{O}_2$ by direct detection of its phosphorescence. The ability to detect $^1\text{O}_2$ generated from sub-picomole quantities of photosensitizer make this approach particularly attractive for the evaluation of newly developed sensitizers from research-scale synthesis. There is also potential for detection of intracellular $^1\text{O}_2$ within the HC-PCF; the feasibility of introducing and trapping cells in the hollow core of HC-PCF has been demonstrated in one of our previous studies.^[38]

The present study has revealed that there are aspects of the HC-PCF technology that can be improved to achieve optimum performance in the present application. The simultaneous, efficient guidance of excitation light and luminescence is challenging, because of their disparate wavelengths. Optimisation of the HC-PCF microstructure is required to achieve fundamental-mode guidance at both wavelengths. This will enhance detection sensitivity, by preferential photosensitization and detection of $^1\text{O}_2$

near the centre of the core where it is not subject to surface-quenching, and facilitate the quantitative photometry that is required for measurement of absolute quantum yields of $^1\text{O}_2$ generation. In the present configuration, the collection of luminescence into the core mode is not very efficient, because of the small collection angle (the small numerical aperture of the fundamental mode). Modification of the fibre structure by the addition of an outer low-index cladding would significantly increase the collection efficiency, as a result of guidance of the $^1\text{O}_2$ emission by total internal reflection at this outer boundary. There is also scope for substantial enhancement of detection sensitivity by surface-modification of the fibre core to inhibit the adsorption of photosensitizer. The ability to functionalise the core surface has been demonstrated previously in the context of monitoring heterogeneous catalysis within HC-PCF.^[39]

We anticipate that a particularly significant future development will be the detection of $^1\text{O}_2$ produced by two-photon-induced photosensitization in HC-PCF. In conventional, cuvette-based experiments, the extremely high, local photon intensity required to achieve two-photon absorption is created by focusing a pulsed laser beam into a spot of about 1 μm in diameter, giving a focal volume of the order of 1 femtolitre. The confinement of two-photon-induced photosensitization to the laser focal point is the basis of its application to achieve high spatial selectivity in photodynamic therapy. Unfortunately, the miniscule excitation volume makes the detection of two-photon-induced $^1\text{O}_2$ generation exceptionally challenging. Although time-resolved detection of $^1\text{O}_2$ luminescence following two-photon photosensitization in bulk solution has been achieved in a few studies, this involves the use of high-power, amplified femtosecond lasers and organic solvents, such as toluene, in which the phosphorescence quantum yield of $^1\text{O}_2$ is relatively high.^[12, 40, 41] The unique optofluidic properties of HC-PCF offer a radically new approach to the study of two-photon induced processes in solution. As we have shown previously, confinement of both laser beam and sample solution within the fibre core permits two-photon excitation to be sustained over a path-length of more than 10 cm.^[28] When combined with the highly sensitive detection of $^1\text{O}_2$ luminescence demonstrated in the present work, this heralds the highly advantageous prospect of a straightforward method for the *in vitro* screening and quantitative characterisation of two-photon photosensitizers, under mechanistically relevant conditions.

Experimental Section

The hollow-core photonic crystal fibres (HC-PCF) were custom-fabricated at the Max Planck Institute for the Science of Light. The photosensitizers, Rose Bengal disodium salt (RB), Hypericin (Hyp) and deuterated solvents, methanol- d_4 (CD_3OD) and deuterium oxide (D_2O) were purchased from Sigma Aldrich, and used as received. In all experiments, deuterated solvents were used to reduce solvent-induced quenching of singlet oxygen phosphorescence,^[27] and solvents were aerated.

The experimental system is shown in Figure 1(d). A 15-cm length of HC-PCF was mounted between a pair of custom-built,

pressurisable cells (as described previously^[23]) to allow introduction of the sample solution into the hollow core, via a syringe pump, whilst maintaining optical alignment and minimising dead volume. For RB, in both D_2O and CD_3OD , significant photo-bleaching was observed for prolonged irradiation of a static solution within the HC-PCF. To prevent this, a continuous flow of solution at a rate of 1 mL per hour was used to replenish the contained volume completely every 30 seconds. Hypericin was less susceptible to photobleaching, allowing the use of longer integration times for signal acquisition.

The 532-nm excitation source was a Nd:YAG laser (Lumanova GmbH, Hannover, Germany) operating at a repetition rate of 3 kHz and a pulse length of 3 ns, with average output power of 8 mW. A variable neutral density filter was used to control the laser intensity. In- and out-coupling of the laser to and from the fibre was performed using objective lenses (4x magnification). The coupling efficiency was approximately 60%, resulting in a laser power of about 1.3 mW within the fibre core. The coupled optical modes were monitored using a CCD camera. At the photosensitizer concentrations used in these experiments, the decrease in excitation intensity along the 15-cm length of the fibre was less than 10%, resulting in essentially homogeneous excitation of the photosensitizer solution along the entire path-length.

The singlet oxygen emission (1270 nm) was spectrally separated from the excitation light and the intrinsic fluorescence of the sensitizer by a long-pass filter (950 nm cut-on, Andover Corp., US) and a band-pass filter centred at 1270 nm (Interferenzoptik Elektronik GmbH, Germany), placed between fibre output and the detector. The large difference in wavelength between the excitation light and the singlet oxygen emission also resulted in spatial filtering, caused by chromatic dispersion from the out-coupling objective. The optical path to the CCD camera was optimised for the detection of the 532-nm, beam, to allow imaging of the excitation mode, whilst the alignment into the objective before the detection fibre was optimised to collect the 1270-nm luminescence. The decay of the singlet oxygen luminescence was measured using a thermoelectrically cooled photomultiplier (model H10330-45, Hamamatsu Photonics Ltd, Hertfordshire, UK) in combination with a photon counting system. A fast photodiode (PDM-400, Becker-Hickl GmbH, Berlin, Germany) was used to synchronize the laser pulse with the photon counting system. The photon counting detection equipment consisted of a multiscaler board with 5-ns resolution and up to 512k channels (model MSA-300, Becker-Hickl GmbH, Berlin, Germany). For integration of the signal traces, the bin width was set at 0.1 μs . Signals were integrated typically over 200,000 laser pulses (1 minute).

Decay curves were analysed using the FAST software package (Edinburgh Instruments Ltd), employing a standard iterative, non-linear least-squares method and assuming a normalised multi-exponential decay function:

$$I(t) = \sum_{i=1}^n A_i \exp\left(-\frac{t}{\tau_i}\right), \quad \sum_{i=1}^n A_i = 1 \quad (1)$$

where A_i is the fractional amplitude and τ_i the lifetime of the i th decay component. As a result of the very low luminescence quantum yield of singlet oxygen, the measured decay curves were distorted at early times ($t < t_f$) by the presence of some residual

sensitizer luminescence. We therefore omitted data-points in the range $0 < t < t_F$ from the fitted function and extrapolated it back in time to $t = 0$ so as to determine the true fractional amplitude for each lifetime component. After some manipulation, this results in the following expression for A_i :

$$A_i = \frac{A_{if} \exp\left(\frac{t_F}{\tau_i}\right)}{\sum_{i=1}^n A_{if} \exp\left(\frac{t_F}{\tau_i}\right)} \quad (2)$$

where A_{if} is the amplitude of the i th component obtained using FAST over the data range $t > t_F$.

The quantum yields of singlet oxygen production, were measured relative to that of RB in D₂O by measuring the relative intensity of the ¹O₂ emission (extrapolated back to time zero) from the different photosensitizer solutions, under identical excitation conditions. During these measurements care was taken to maintain alignment of the laser into the fibre, observed via the camera, during filling and flushing of the fibre core. Complete cleaning of the fibre between samples was confirmed by measuring for several minutes until the luminescence counts had dropped to zero.

The 60-μm core diameter of the HC-PCF used here was larger than that of the fibres we have used in previous studies (10–20 μm).^[25, 26, 28] this enabled guiding of a wide range of wavelengths, encompassing the excitation light and near-infrared luminescence, but coupling efficiencies were lower and guidance losses higher than for smaller-core fibres of this type. Moreover, achieving and maintaining a single fundamental mode for excitation was difficult, as shown by Figure 1(c). To minimise these difficulties, the fibre was kept as straight as possible throughout the experiment. Whilst the overall coupling efficiency achieved was acceptable, the presence of higher order modes resulted in significant excitation intensity at the perimeter of the fibre core and consequent excitation of surface-deposited sensitizer molecules. Work is ongoing to produce fibres with guidance properties optimised for this application.

Acknowledgements

We are grateful to the EPSRC (UK) for financial support in the form of a Doctoral Prize Scholarship for GOSW. The research data supporting this publication can be accessed at <URL to be inserted>.

Keywords: singlet oxygen, luminescence, photonic crystal fibre, photosensitization, lifetime.

- [1] P. R. Ogilby *Chem. Soc. Rev.* **2010**, 39, 3181–3209.
- [2] H. Y. Wu, Q. J. Song, G. X. Ran, X. M. Lu, B. G. Xu *Trac-Trends in Analytical Chemistry*. **2011**, 30, 133–141.
- [3] R. Schmidt *Photochem. Photobiol.* **2006**, 82, 1161–1177.
- [4] P. Agostinis, K. Berg, K. A. Cengel, T. H. Foster, A. W. Girotti, S. O. Gollnick, S. M. Hahn, M. R. Hamblin, A. Juzeniene, D. Kessel, M. Korbelik, J. Moan, P. Mroz, D. Nowis, J. Piette, B. C. Wilson, J. Golab *CA Cancer J Clin.* **2011**, 61, 250–281.
- [5] B. Li, L. Lin, H. Lin, B. C. Wilson *J Biophotonics*. **2016**, 9, 1314–1325.
- [6] H. Abrahamse, M. R. Hamblin *Biochem. J.* **2016**, 473, 347–364.
- [7] P. Rishi, E. Rishi, M. Bhende, V. Agarwal, C. H. Vyas, M. Valiveti, P. Bhende, C. Rao, P. Susvar, P. Sen, R. Raman, V. Khetan, V. Murali, D. Ratra, T. Sharma *Br J Ophthalmol.* **2016**, 100, 1337–1340.
- [8] J. Chen, T. C. Cesario, P. M. Rentzepis *Proc Natl Acad Sci U S A.* **2014**, 111, 33–38.
- [9] S. Noimark, E. Salvadori, R. Gomez-Bombarelli, A. J. MacRobert, I. P. Parkin, C. W. Kay *Phys. Chem. Chem. Phys.* **2016**, 18, 28101–28109.
- [10] M. R. Hamblin *Curr Opin Microbiol.* **2016**, 33, 67–73.
- [11] T. Gallavardin, C. Armagnat, O. Maury, P. L. Baldeck, M. Lindgren, C. Monnerneau, C. Andraud *Chem Commun.* **2012**, 48, 1689–1691.
- [12] S. P. McIlroy, E. Clo, L. Nikolajsen, P. K. Frederiksen, C. B. Nielsen, K. V. Mikkelsen, K. V. Gothelf, P. R. Ogilby *J. Org. Chem.* **2005**, 70, 1134–1146.
- [13] Y. Shen, A. J. Shuhendler, D. Ye, J. J. Xu, H. Y. Chen *Chem. Soc. Rev.* **2016**, 45, 6725–6741.
- [14] X. Tian, Y. Zhu, M. Zhang, L. Luo, J. Wu, H. Zhou, L. Guan, G. Battaglia, Y. Tian *Chem Commun.* **2017**, 53, 3303–3306.
- [15] A. Jimenez-Banzo, X. Ragas, P. Kapusta, S. Nonell *Photochem Photobiol Sci.* **2008**, 7, 1003–1010.
- [16] N. R. Gemmell, A. McCarthy, B. Liu, M. G. Tanner, S. D. Dorenbos, V. Zwiller, M. S. Patterson, G. S. Buller, B. C. Wilson, R. H. Hadfield *Opt. Express*. **2013**, 21, 5005–5013.
- [17] G. Boso, D. Ke, B. Korzh, J. Bouilloux, N. Lange, H. Zbinden *Biomed Opt Express*. **2016**, 7, 211–224.
- [18] N. R. Gemmell, A. McCarthy, M. M. Kim, I. Veilleux, T. C. Zhu, G. S. Buller, B. C. Wilson, R. H. Hadfield *J Biophotonics*. **2017**, 10, 320–326.
- [19] X. Li, G. Zhang, H. Ma, D. Zhang, J. Li, D. Zhu *J. Am. Chem. Soc.* **2004**, 126, 11543–11548.
- [20] L. A. MacManus-Spencer, D. E. Latch, K. M. Kroncke, K. McNeill *Anal. Chem.* **2005**, 77, 1200–1205.
- [21] S. K. Pedersen, J. Holmehave, F. H. Blaikie, A. Gollmer, T. Breitenbach, H. H. Jensen, P. R. Ogilby *J. Org. Chem.* **2014**, 79, 3079–3087.
- [22] B. Song, G. Wang, J. Yuan *Chem Commun.* **2005**, 3553–3555.
- [23] A. M. Cubillas, S. Unterkofler, T. G. Euser, B. J. Etzold, A. C. Jones, P. J. Sadler, P. Wasserscheid, P. St.J. Russell *Chem. Soc. Rev.* **2013**, 42, 8629–8648.
- [24] P. Russell *Science*. **2003**, 299, 358–362.
- [25] G. O. S. Williams, T. G. Euser, P. St.J. Russell, A. C. Jones, *Methods Appl. Fluoresc.* **2013**, 1, 015003.
- [26] G. O. S. Williams, J. S. Chen, T. G. Euser, P. St.J. Russell, A. C. Jones *Lab Chip*. **2012**, 12, 3356–3361.
- [27] M. Bregnhøj, M. Westberg, F. Jensen, P. R. Ogilby *Phys. Chem. Chem. Phys.* **2016**, 18, 22946–22961.
- [28] G. O. S. Williams, T. G. Euser, J. Arlt, P. St.J. Russell, A. C. Jones *ACS Photonics*. **2014**, 1, 790–793.
- [29] M. Y. Li, C. S. Cline, E. B. Koker, H. H. Carmichael, C. F. Chignell, P. Bilski *Photochem. Photobiol.* **2007**, 74, 760–764.
- [30] F. Wilkinson, W. P. Helman, A. B. Ross *J. Phys. Chem. Ref. Data*. **1995**, 24, 663–1021.
- [31] T. Daimon, Y. Nosaka *J. Phys. Chem. C* **2007**, 111, 4420–4424.
- [32] J. S. Y. Chen, PhD Thesis, University of Erlangen-Nuremberg (2010).
- [33] M. E. Daraio, E. San Roman *Helv. Chim. Acta.* **2001**, 84, 2601–2614.
- [34] S. H. Behrens, D. G. Grier *J. Chem. Phys.* **2001**, 115, 6716–6721.
- [35] A. K. Coker, Ludwig's Applied Process Design for Chemical and Petrochemical Plants (Fourth Edition), Elsevier, **2014**.
- [36] F. Ruyffelaere, V. Nardello, R. Schmidt, J. M. Aubry *J. Photochem. Photobiol. A* **2006**, 183, 98–105.
- [37] F. Wilkinson, W. P. Helman, A. B. Ross *J. Phys. Chem. Ref. Data*. **1993**, 22, 113–262.
- [38] S. Unterkofler, M. K. Garbos, T. G. Euser, J. R. P. St J *Biophotonics*. **2013**, 6, 743–752.
- [39] A. M. Cubillas, M. Schmidt, T. G. Euser, N. Taccardi, S. Unterkofler, P. S. Russell, P. Wasserscheid, B. J. M. Etzold *Adv. Mater. Interfaces*. **2014**, 1, 1300093–1300097.

- [40] J. Arnbjerg, M. Johnsen, P. K. Frederiksen, S. E. Braslavsky, P. R. Ogilby
J. Phys. Chem. A, **2006**, 110, 7375-7385.
- [41] P. R. Ogilby in *Singlet Oxygen: Applications in Biosciences and Nanosciences, Vol. 1* (Eds.: S. Nonell, C. Flors), The Royal Society of Chemistry, **2016**, pp.145-161.
-

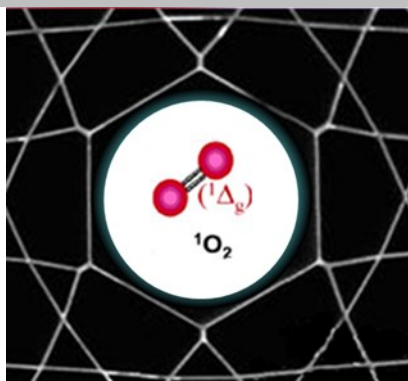
ARTICLE

Entry for the Table of Contents (Please choose one layout)

Layout 1:

ARTICLE

Core benefits: we describe the use of hollow-core photonic crystal fibre as an optofluidic microreactor for generation and detection of singlet oxygen. Excitation of photosensitizer solution within the hollow core of the optical fibre enables detection of singlet oxygen with sub-picomole sensitivity by time-resolved measurement of its intrinsic phosphorescence.



Gareth O.S. Williams, Tijmen G. Euser,
Philip St.J. Russell, Alexander J.
MacRobert* and Anita C. Jones*

Page No. – Page No.

**Highly sensitive luminescence
detection of photosensitized singlet
oxygen within photonic crystal fibre**

Highly sensitive luminescence detection of photosensitized singlet oxygen within photonic crystal fibre

Gareth O.S. Williams¹, Tijmen G. Euser^{2,3}, Philip St.J. Russell², Alexander J. MacRobert^{4*} and Anita C. Jones^{1*}

¹EaStCHEM School of Chemistry, Joseph Black Building, The University of Edinburgh, Edinburgh, EH9 3FJ, UK. ²Max-Planck Institute for the Science of Light, Staudtstr 2, 91058 Erlangen, Germany.

³Current address: NanoPhotonics Centre, Cavendish Laboratory, University of Cambridge, J. J. Thomson Avenue, Cambridge CB3 0HE, UK. ⁴Division of Surgery & Interventional Science, University College London, Charles Bell House, London W1WJN, UK.

Supporting Information

Calculation of the diffusion coefficient of ¹O₂ in CD₃OD.

An experimental value could not be found in the literature, so the value was calculated by the Wilke-Chang method, using the Excel spreadsheet provided as Supplementary Material by Coker^[1], Ludwig's Applied Process Design for Chemical and Petrochemical Plants, 4th Edition, Elsevier 2014, (ISBN: 9780080942421), which can be found at:

<http://booksite.elsevier.com/9780750685245/downloads/liquid-phase-diffusion-coefficient.xls>.

$$D_{AB}^0 = \frac{1.713 \times 10^{-13} (\phi M_{w,B})^{0.5} T}{\mu_B \cdot v_A^{0.6}}$$

where D_{AB}^0 is the diffusion coefficient of solute A at very low concentration (<5-10 mole%) in solvent B (m²/s); $M_{w,B}$ is the molecular weight of solvent B; μ_B is the viscosity of solvent B, (mN s/m²); v_A is the molar volume of solute A at its normal boiling temperature (m³/kmol); ϕ is the association factor of solvent B (dimensionless).

Values used were: ϕ (methanol) = 1.9, μ_B (methanol) = 0.594 mN s/m²; v_A (O₂) = 0.0256 m³/kmol; T = 293.15 K.

This gave a value of D_{AB}^0 for O₂ in CD₃OD of 4.3x10⁻⁹ m²s⁻¹.

For verification, the analogous calculation for O₂ in H₂O gave a value of 2.1x10⁻⁹ m²s⁻¹, which is in good agreement with experimental values in the literature^[2] of ~2x10⁻⁹ m²s⁻¹.

References

- [1] A. K. Coker, Ludwig's Applied Process Design for Chemical and Petrochemical Plants (Fourth Edition), Elsevier, **2014**.
- [2] M. Tsushima, K. Tokuda, T. Ohsaka *Analytical Chemistry*. **1994**, 66, 4551-4556.